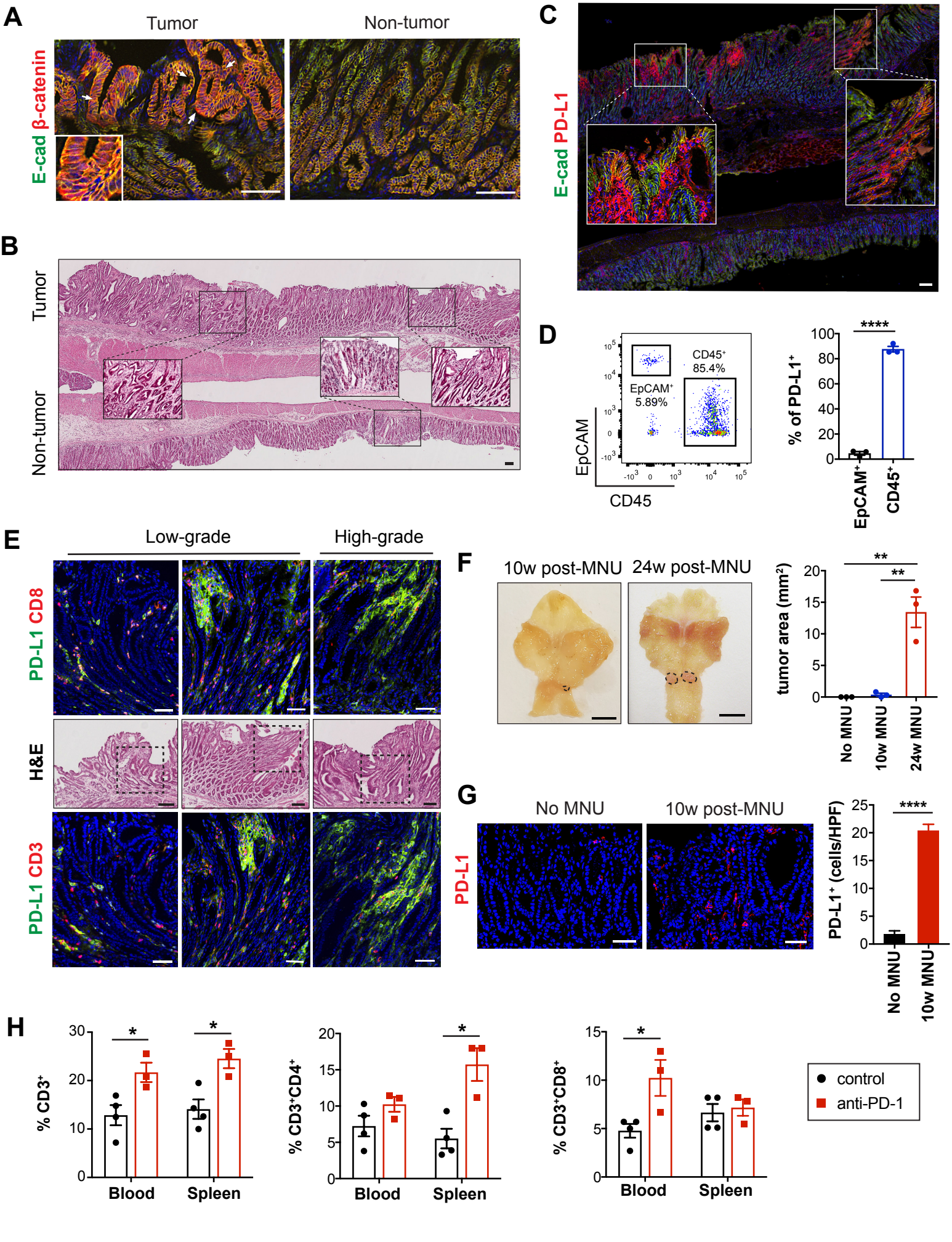
A
Tumor
Non-tumor
E-cad β-catenin
B
Tumor
Non-tumor
C
E-cad PD-L1
D
CD45⁺ 85.4%
EpCAM⁺ 5.89%
EpCAM
CD45
% of PD-L1⁺
****
EpCAM⁺
CD45⁺
E
Low-grade
High-grade
PD-L1 CD8
H&E
PD-L1 CD3
F
10w post-MNU
24w post-MNU
tumor area (mm²)
**
**
No MNU
10w MNU
24w MNU
G
No MNU
10w post-MNU
PD-L1
PD-L1⁺ (cells/HPF)
****
No MNU
10w MNU
H
% CD3⁺
% CD3⁺CD4⁺
% CD3⁺CD8⁺
*
Blood
Spleen
control
anti-PD-1

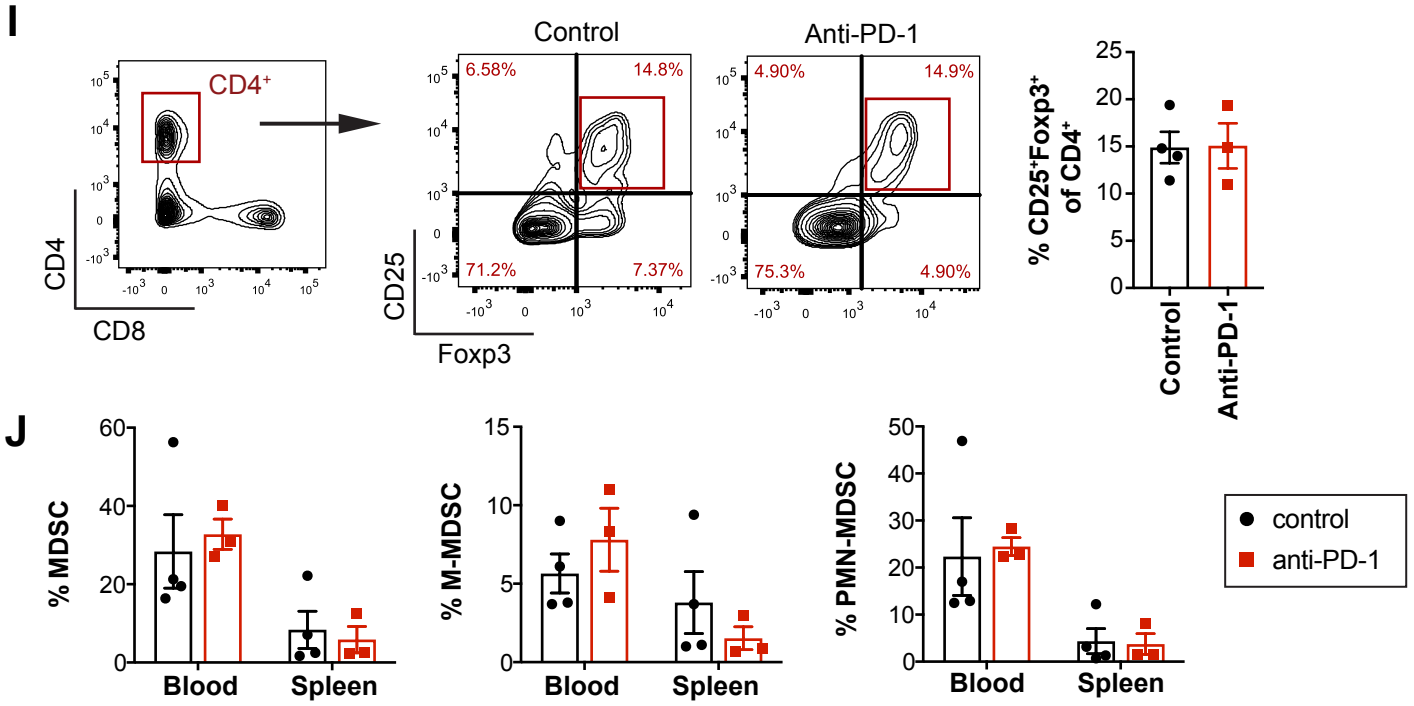

Figure S1. Early treatment of PD-1 blockade in *Hf*/MNU/GAS-KO mice

(A) Immunostaining for β-catenin and E-cadherin on gastric tissue from *Hf*/MNU-induced GAS-KO mice at 30 weeks post-MNU. Arrows indicate nuclear β-catenin. Scale bar, 100 μm.

(B) H&E stain of gastric tissue from GAS-KO mice at 30 weeks post-MNU. Scale bar, 100 μm.

(C) Confocal microscopy image of gastric tissue stained for E-cadherin and PD-L1 in GAS-KO mice at 30 weeks post-MNU. Scale bar, 100 μm.

(D) Flow cytometric analysis of the percentage of PD-L1$^+$ cells in EpCAM$^+$ epithelial cells and CD45$^+$ leukocytes isolated from GAS-KO tumors at 30 weeks post-MNU (n = 3).

(E) *Hf*/MNU/GAS-KO tumors co-stained with PD-L1 and either CD3 or CD8 and corresponding H&E stains. Scale bar, 50 μm for immunostaining; 100 μm for H&E stain.

(F) Gross images and tumor area measured in *Hf*/MNU/GAS-KO mice at 10 and 24 weeks post-MNU and control animals without *Hf*/MNU induction (n = 3 per group). Dotted lines indicate tumor area.

(G) PD-L1 immunostaining on gastric tissues from GAS-KO mice at 10 weeks post-MNU and control animals without *Hf*/MNU induction, and quantification of PD-L1$^+$ cells (n = 3/group).

(H) The percentage of CD3$^+$, CD4$^+$ and CD8$^+$ T cells in the peripheral blood and spleen from GAS-KO mice treated with isotype control (n = 4) or anti-PD-1 (n = 3).

(I) Representative contour plots to gate CD4$^+$CD25$^+$Foxp3$^+$ Tregs in spleen and quantification of the percentage of CD25$^+$Foxp3$^+$ cells in CD4$^+$ T cells from control (n = 4) and anti-PD-1-treated (n = 3) GAS-KO mice.

(J) The proportion of circulating and splenic MDSCs (CD11b$^+$Gr-1$^+$), M-MDSCs (CD11b$^+$Ly6C^{hi}Ly6G$^-$) and PMN-MDSCs (CD11b$^+$Ly6C^{lo}Ly6G$^+$) in GAS-KO mice treated with IgG control (n = 4) and anti-PD-1 (n = 3).

Data are represented as mean ± SEM. Student's t-test. *P < .05; **P < .01; ****P < .0001.

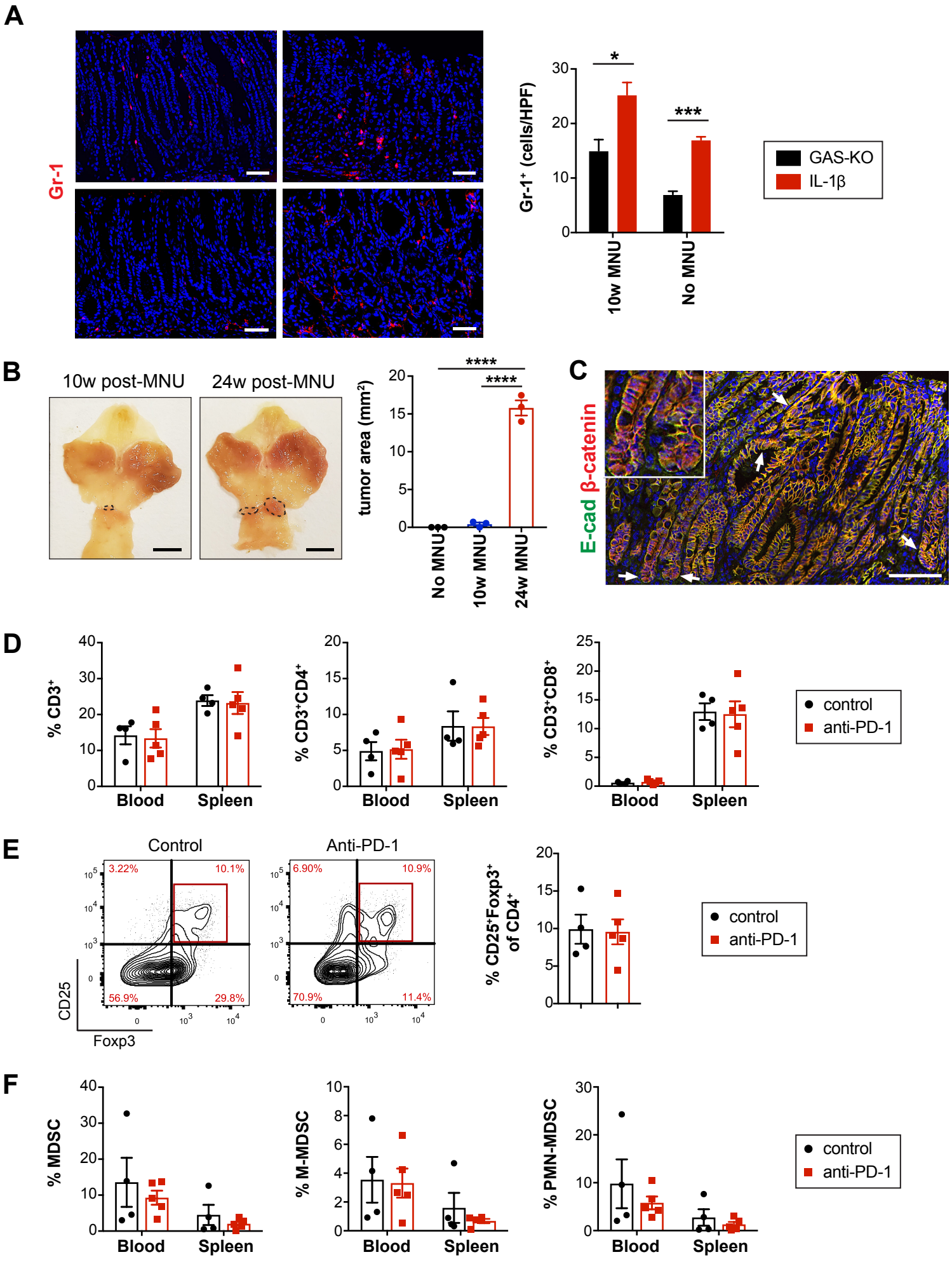
A
Gr-1
Gr-1+ (cells/HPF)
30
20
10
0
*
***
10w MNU
No MNU
GAS-KO
IL-1β
B
10w post-MNU
24w post-MNU
tumor area (mm2)
20
15
10
5
0
****
****
No MNU
10w MNU
24w MNU
C
E-cad β-catenin
D
% CD3+
% CD3+CD4+
% CD3+CD8+
40
30
20
10
0
20
15
10
5
0
25
20
15
10
5
0
Blood
Spleen
control
anti-PD-1
E
Control
Anti-PD-1
3.22%
10.1%
56.9%
29.8%
6.90%
10.9%
70.9%
11.4%
CD25
Foxp3
% CD25+Foxp3+ of CD4+
20
15
10
5
0
control
anti-PD-1
F
% MDSC
% M-MDSC
% PMN-MDSC
40
30
20
10
0
10
8
6
4
2
0
30
20
10
0
Blood
Spleen
control
anti-PD-1

Figure S2. H/K-ATPase-IL-1β mice with anti-PD-1 in the early treatment regimen

(A) Gr-1 immunostaining on gastric tissues from *Hf*/MNU-induced GAS-KO and IL-1β mice at 10 weeks post-MNU and control animals without *Hf*/MNU, and quantification of Gr-1$^+$ cells.

(B) Gross images and tumor area measured in *Hf*/MNU/IL-1β mice at 10 and 24 weeks post-MNU and control animals without *H. felis*/MNU induction (n = 3/group). Dotted lines indicate tumor area. Scale bars, 5 mm.

(C) Immunostaining for β-catenin and E-cadherin on *Hf*/MNU/IL-1β tumors at 30 weeks post-MNU. Arrows indicate nuclear β-catenin. Scale bar, 100 μm.

(D) The percentage of circulating and splenic total CD3$^+$ T cells and CD4$^+$ and CD8$^+$ T cell subsets in control (n = 4) and anti-PD-1-treated (n = 5) IL-1β mice.

(E) Representative contour plots showing CD25$^+$Foxp3$^+$ cells gated on CD4$^+$ cells and quantification in splenic tissue from IL-1β mice following control (n = 4) and anti-PD-1 treatment (n = 5).

(F) The proportion of total MDSCs (CD11b$^+$Gr-1$^+$), M-MDSCs (CD11b$^+$Ly6C^{hi}Ly6G$^-$), and PMN-MDSCs (CD11b$^+$Ly6C^{lo}Ly6G$^+$) in the peripheral blood and spleen from control (n = 4) and anti-PD-1-treated (n = 5) IL-1β mice.

Data are represented as mean ± SEM. Student's t-test. *P < .05; ***P < .001; ****P < .0001.

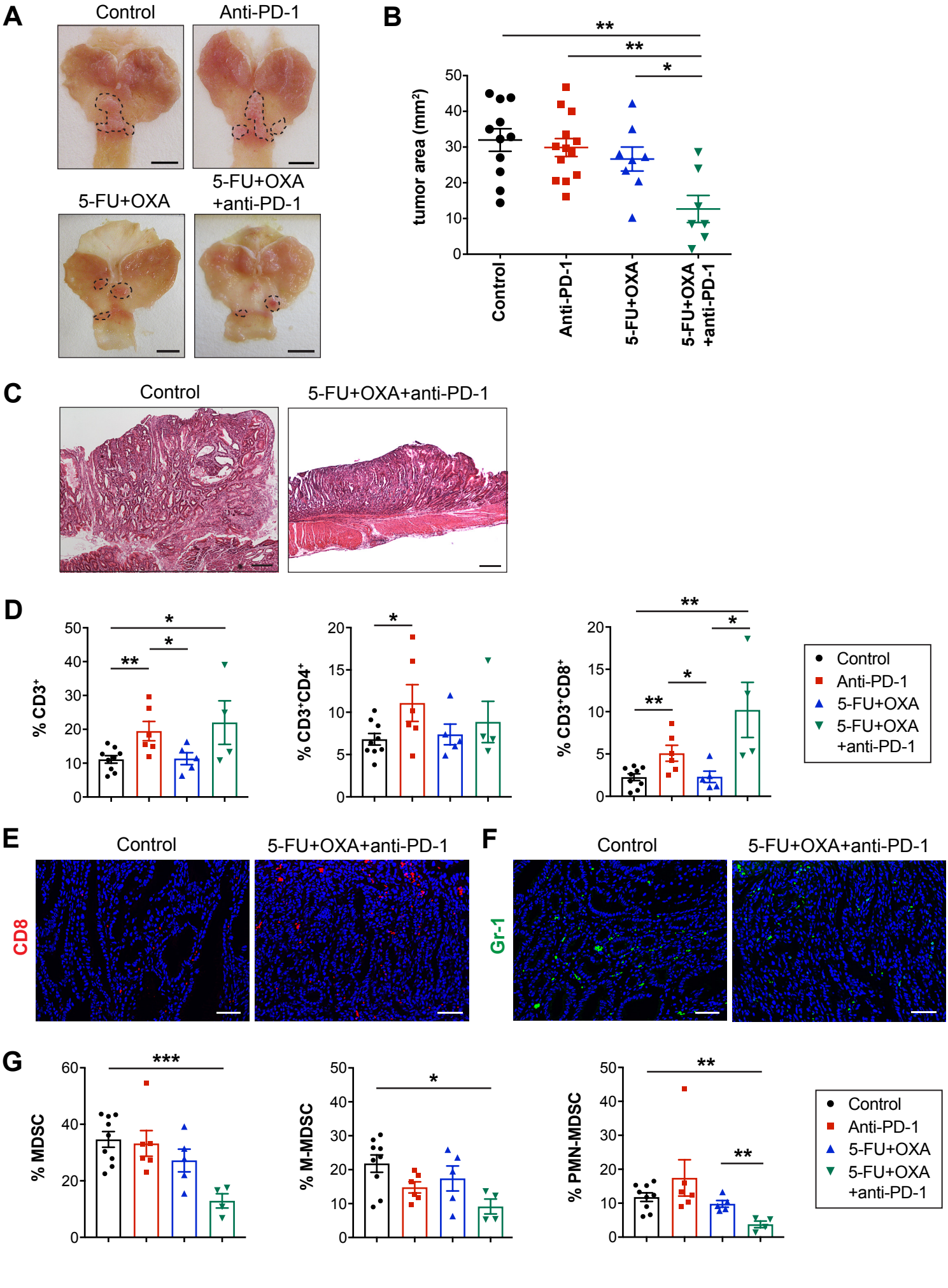
A
Control
Anti-PD-1
5-FU+OXA
5-FU+OXA +anti-PD-1
B
tumor area (mm²)
Control
Anti-PD-1
5-FU+OXA
5-FU+OXA +anti-PD-1
C
Control
5-FU+OXA+anti-PD-1
D
% CD3⁺
% CD3⁺CD4⁺
% CD3⁺CD8⁺
Control
Anti-PD-1
5-FU+OXA
5-FU+OXA +anti-PD-1
E
Control
5-FU+OXA+anti-PD-1
CD8
F
Control
5-FU+OXA+anti-PD-1
Gr-1
G
% MDSC
% M-MDSC
% PMN-MDSC
Control
Anti-PD-1
5-FU+OXA
5-FU+OXA +anti-PD-1

Figure S3. Chemotherapy in combination with PD-1 blockade significantly decreases tumor burden in H/K-ATPase-IL-1β mice.

(A-B) Gross images of gastric tissue (A) and tumor area measured (B) from IL-1β mice treated with isotype control (n = 11), anti-PD-1 alone (n = 13), chemotherapy (5-FU + OXA) alone (n = 8), and chemotherapy in combination with anti-PD-1 (n = 7). Scale bars, 5 mm (A). One-way ANOVA (B).

(C) H&E stains of IL-1β tumors treated with isotype control or combined anti-PD-1 with chemothrapy. Scale bars, 200 μm.

(D) The percentage of tumor-infiltrating total $CD3^+$ T cells and $CD4^+$ and $CD8^+$ T cell subsets from IL-1β mice with control (n = 9), anti-PD-1 alone (n = 6), chemotherapy alone (n = 5), and combination treatment (n = 4). Student's t-test.

(E-F) Immunofluorescence staining for CD8 (E) and Gr-1(F) on IL-1β tumors treated with isotype control or combined anti-PD-1 with chemotherapy. Scale bars, 50 μm.

(G) The percentage of total MDSCs, M-MDSCs, and PMN-MDSCs in IL-1β tumors treated as indicated. Student's t-test.

Data are represented as mean ± SEM. $*P < .05$; $**P < .01$; $***P < .001$.

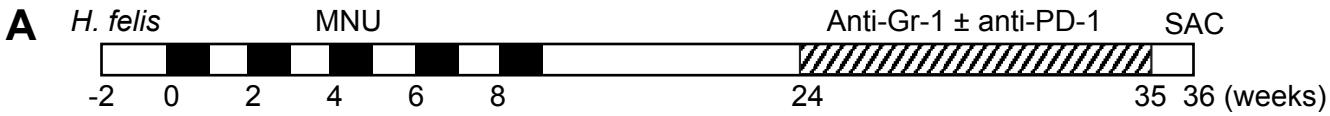
A
H. felis
MNU
Anti-Gr-1 ± anti-PD-1
SAC
-2
0
2
4
6
8
24
35
36 (weeks)

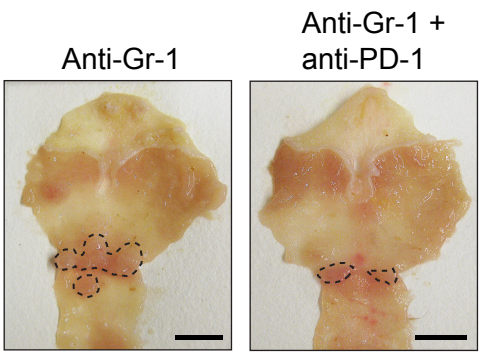
B
Anti-Gr-1
Anti-Gr-1 +
anti-PD-1

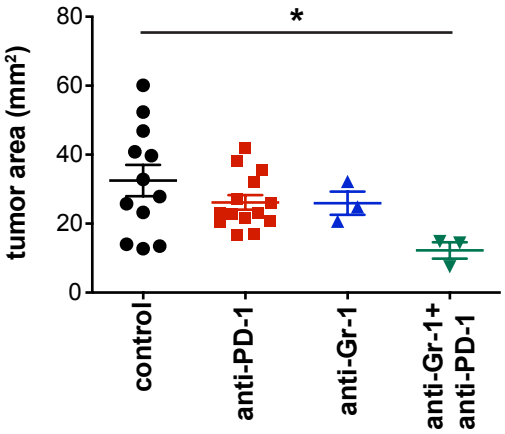
C
tumor area (mm²)
control
anti-PD-1
anti-Gr-1
anti-Gr-1+
anti-PD-1

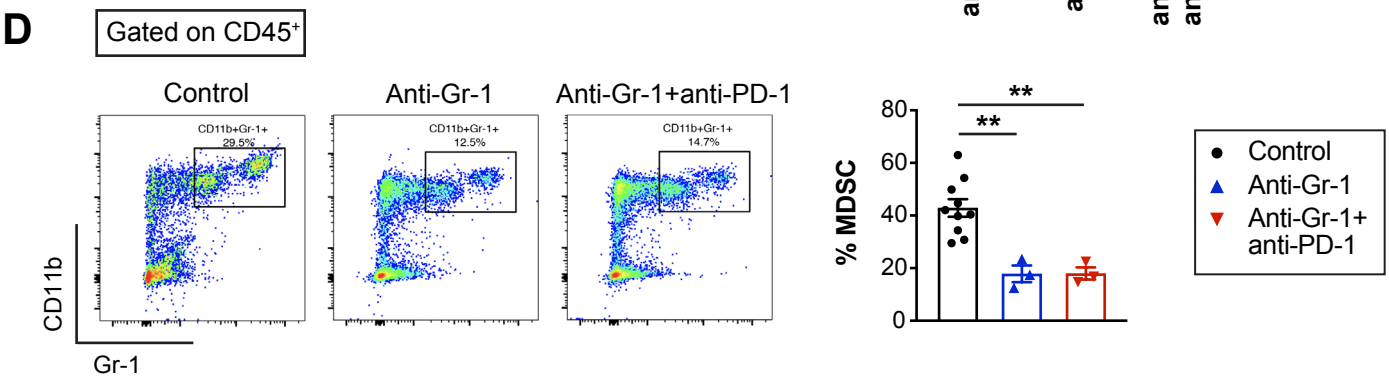
D
Gated on CD45⁺
Control
Anti-Gr-1
Anti-Gr-1+anti-PD-1
CD11b
Gr-1
% MDSC
Control
Anti-Gr-1
Anti-Gr-1+
anti-PD-1

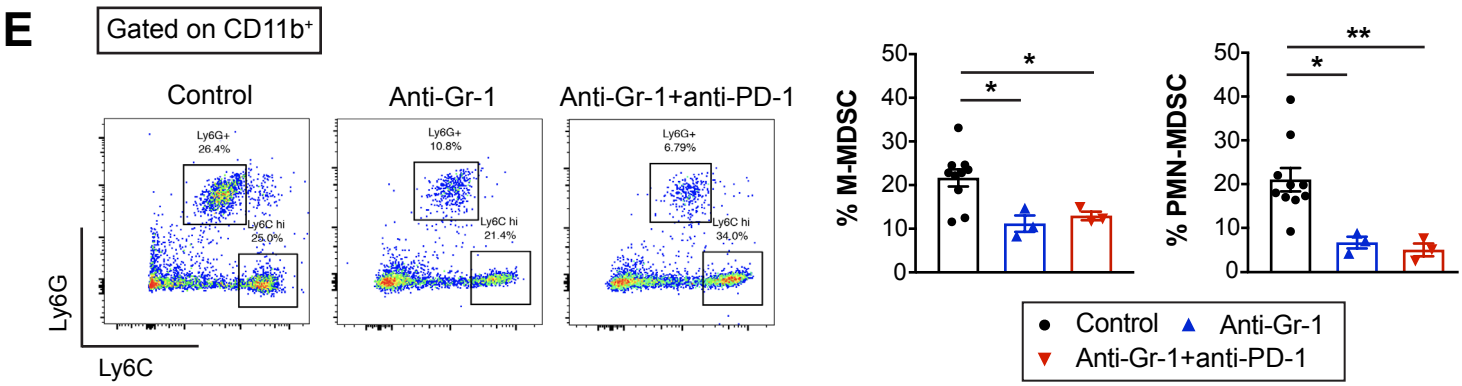
E
Gated on CD11b⁺
Control
Anti-Gr-1
Anti-Gr-1+anti-PD-1
Ly6G
Ly6C
% M-MDSC
% PMN-MDSC
Control
Anti-Gr-1
Anti-Gr-1+anti-PD-1

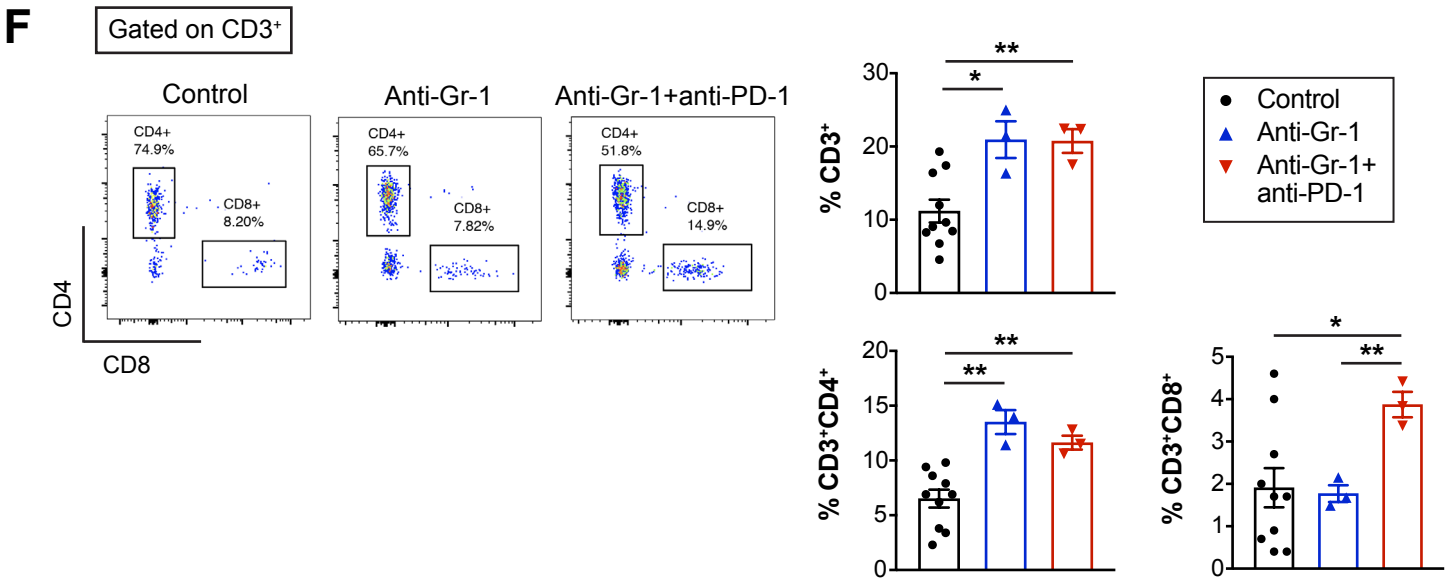
F
Gated on CD3⁺
Control
Anti-Gr-1
Anti-Gr-1+anti-PD-1
CD4
CD8
% CD3⁺
% CD3⁺CD4⁺
% CD3⁺CD8⁺
Control
Anti-Gr-1
Anti-Gr-1+
anti-PD-1

Figure S4. The combination of anti-Gr-1 and anti-PD-1 inhibits gastric tumor growth in GAS-KO mice

(A) Experimental scheme depicting induction of gastric cancer by *Hf*/MNU and treatment with anti-Gr-1 in combination with anti-PD-1.

(B) Gross findings of GAS-KO mice treated with anti-Gr-1 alone or in combination with anti-PD-1. Scale bars, 5 mm.

(C) Measured tumor area from GAS-KO mice in the different treatment groups. Control and anti-PD-1 alone groups were previously shown in Figure 3C. Control (n = 12); anti-PD-1 alone (n = 14); anti-Gr-1 alone (n = 3); combination of anti-Gr-1 plus anti-PD-1 (n = 3). One-way ANOVA.

(D-F) Representative flow cytometry plots and quantification showing the percentage of MDSCs (D), MDSC subsets (E), and T cells (F) among $CD45^+$ cells in GAS-KO tumors treated with isotype control, anti-Gr-1 alone or anti-Gr-1 plus anti-PD-1 combination treatment. Student's t-test.

Data are represented as mean ± SEM. **P* < .05; ***P* < .01.

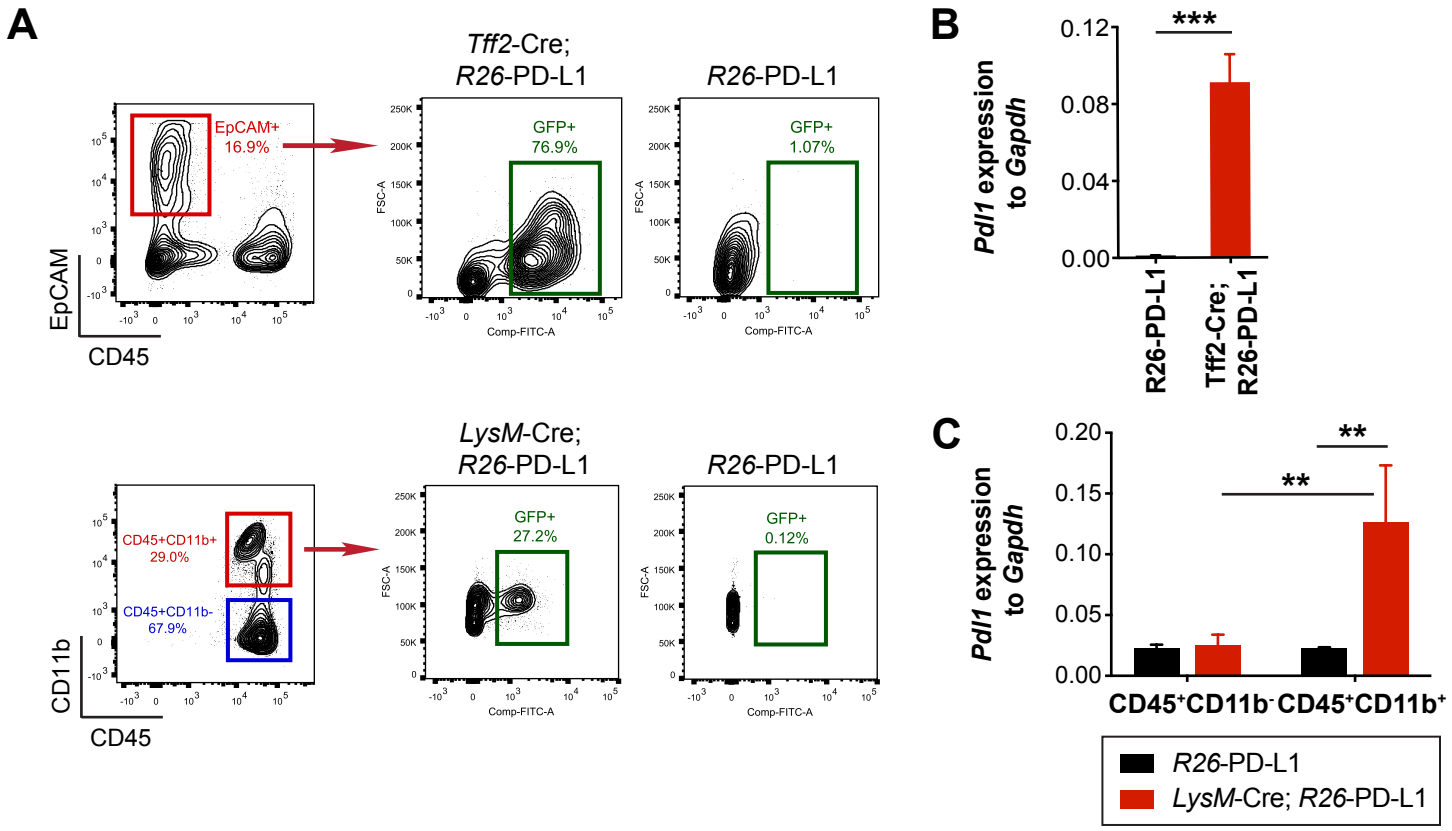
A
Tff2-Cre; R26-PD-L1
R26-PD-L1
EpCAM+ 16.9%
GFP+ 76.9%
GFP+ 1.07%
EpCAM
CD45
LysM-Cre; R26-PD-L1
R26-PD-L1
CD45+CD11b+ 29.0%
CD45+CD11b- 67.9%
GFP+ 27.2%
GFP+ 0.12%
CD11b
CD45
FSC-A
Comp-FITC-A
B
Pdl1 expression to Gapdh
0.12
0.08
0.04
0.00
***
R26-PD-L1
Tff2-Cre; R26-PD-L1
C
Pdl1 expression to Gapdh
0.20
0.15
0.10
0.05
0.00
**
**
CD45+CD11b- CD45+CD11b+
R26-PD-L1
LysM-Cre; R26-PD-L1

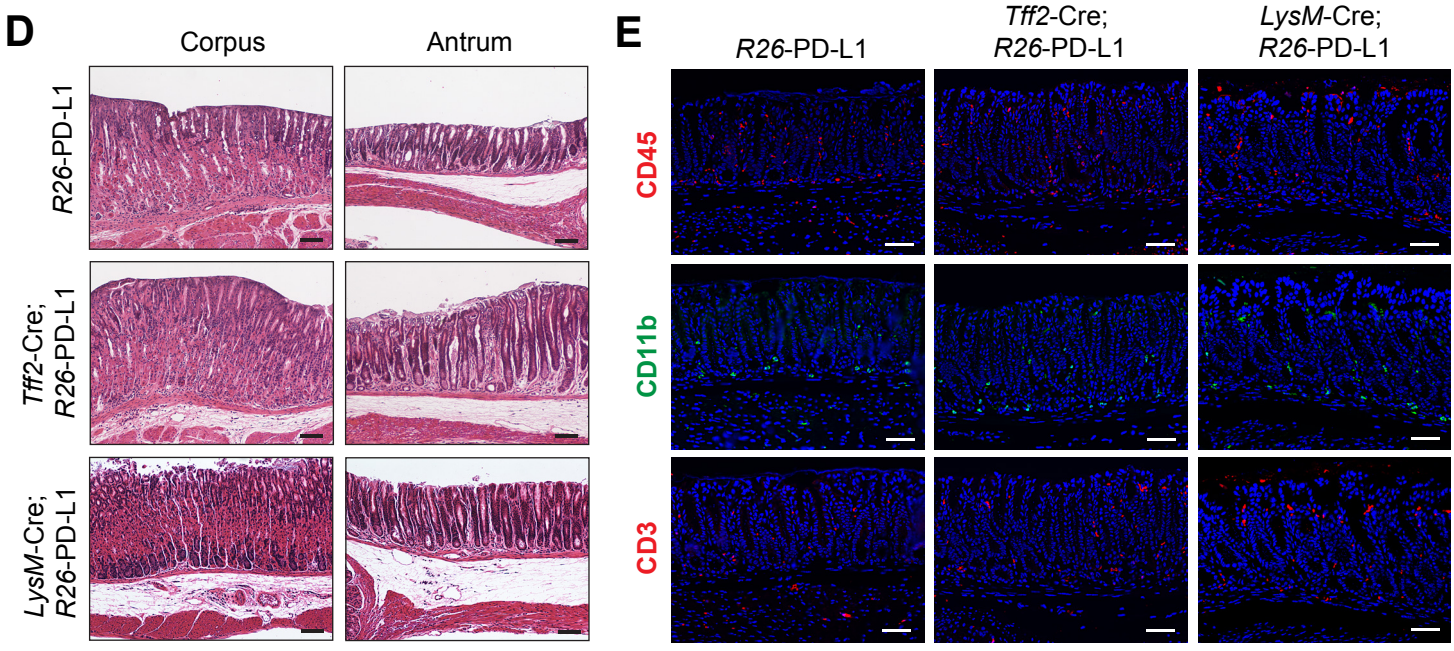
D
Corpus
Antrum
R26-PD-L1
Tff2-Cre; R26-PD-L1
LysM-Cre; R26-PD-L1
E
R26-PD-L1
Tff2-Cre; R26-PD-L1
LysM-Cre; R26-PD-L1
CD45
CD11b
CD3

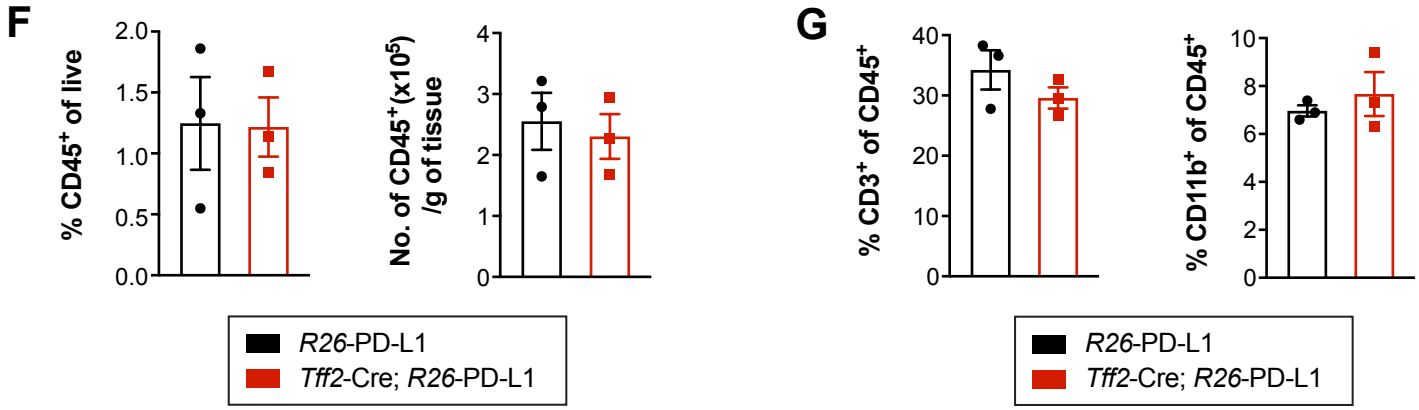
F
% CD45+ of live
2.0
1.5
1.0
0.5
0.0
No. of CD45+(x10^5) /g of tissue
4
3
2
1
0
R26-PD-L1
Tff2-Cre; R26-PD-L1
G
% CD3+ of CD45+
40
30
20
10
0
% CD11b+ of CD45+
10
8
6
4
2
0
R26-PD-L1
Tff2-Cre; R26-PD-L1

Figure S5. Generation of *R26*-LSL-*Pdl1*-EGFP mice

(A) Representative gating and sorting strategy for isolation of epithelial and immune cells from antral tissues in *R26*-PD-L1, *Tff2*-Cre; *R26*-PD-L1, and *LysM*-Cre; *R26*-PD-L1 mice.

(B-C) *Pdl1* gene expression by qPCR in $EpCAM^+$ cells isolated from antral tissues in *R26*-PD-L1 and *Tff2*-Cre; *R26*-PD-L1 mice (B) and in $CD11b^-$ and $CD11b^+$ cells isolated from splenic tissues in *R26*-PD-L1 and *LysM*-Cre; *R26*-PD-L1 mice (n = 3/group).

(D) H&E stains of gastric tissues from *R26*-PD-L1, *Tff2*-Cre; *R26*-PD-L1, and *LysM*-Cre; *R26*-PD-L1 mice at 56 weeks of age. Scale bars, 100 μm.

(E) Immunostaining for CD45, CD11b, and CD3 on gastric tissues from *R26*-PD-L1, *Tff2*-Cre; *R26*-PD-L1 and *LysM*-Cre; *R26*-PD-L1 mice at 56 weeks of age. Scale bars, 50 μm.

(F) The proportion of $CD45^+$ cells in live cells and the absoute number of $CD45^+$ cells in antral tissues from 56-week-old *R26*-PD-L1 and *Tff2*-Cre; *R26*-PD-L1 mice (n = 3/group).

(G) The percentage of $CD3^+$ T cells and $CD11b^+$ myeloid cells among $CD45^+$ cells in antral tissues from 56-week-old *R26*-PD-L1 and *Tff2*-Cre; *R26*-PD-L1 mice (n = 3/group).

Data are represented as mean ± SEM. Student's t-test. $^{**}P < .01$; $^{***}P < .001$.

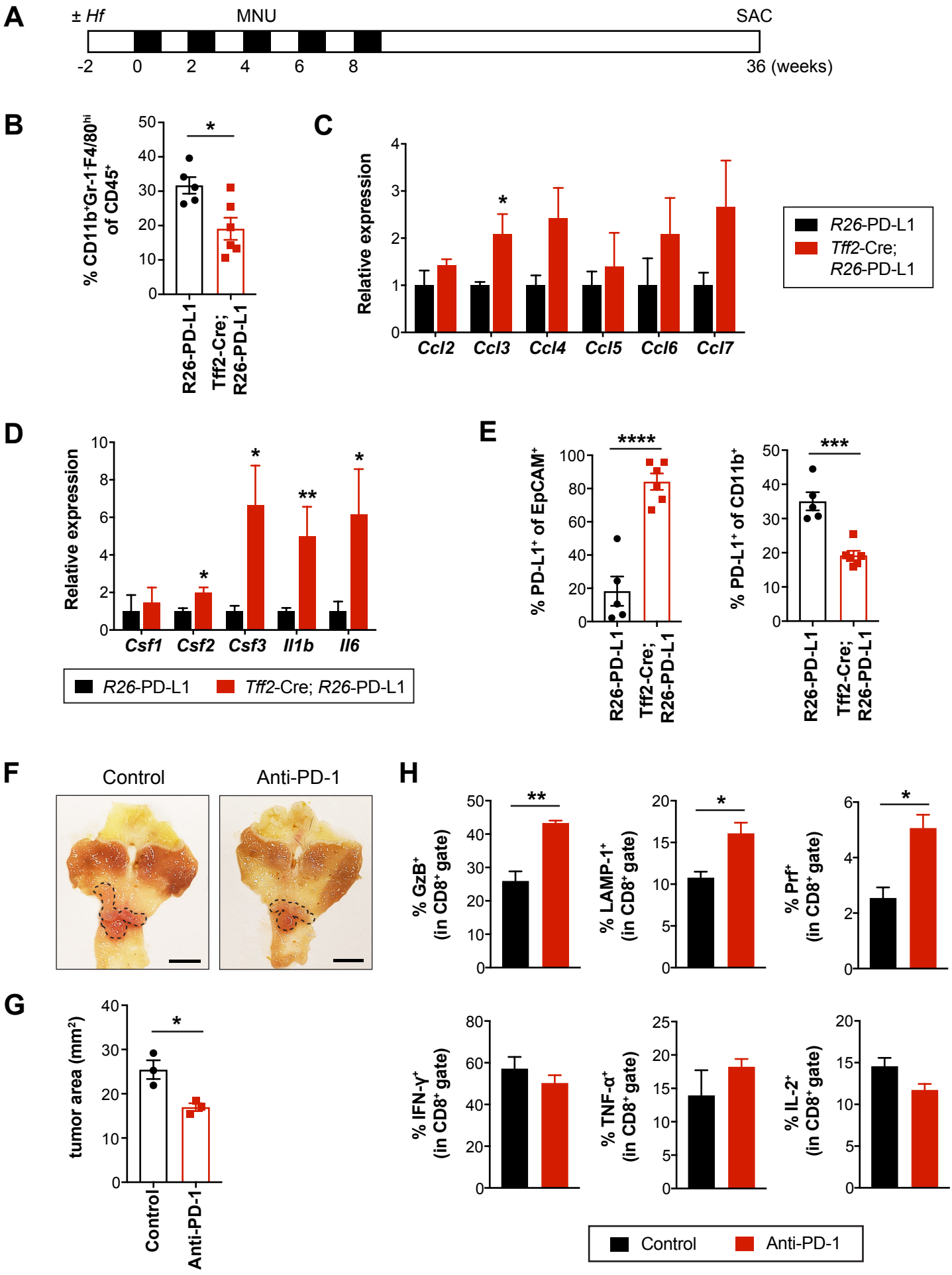
A
± Hf
MNU
SAC
-2
0
2
4
6
8
36 (weeks)
B
% CD11b+Gr-1+F4/80hi of CD45+
R26-PD-L1
Tff2-Cre; R26-PD-L1
C
Relative expression
Ccl2
Ccl3
Ccl4
Ccl5
Ccl6
Ccl7
R26-PD-L1
Tff2-Cre; R26-PD-L1
D
Relative expression
Csf1
Csf2
Csf3
Il1b
Il6
R26-PD-L1
Tff2-Cre; R26-PD-L1
E
% PD-L1+ of EpCAM+
% PD-L1+ of CD11b+
R26-PD-L1
Tff2-Cre; R26-PD-L1
F
Control
Anti-PD-1
G
tumor area (mm2)
Control
Anti-PD-1
H
% GzB+ (in CD8+ gate)
% LAMP-1+ (in CD8+ gate)
% Prf+ (in CD8+ gate)
% IFN-γ+ (in CD8+ gate)
% TNF-α+ (in CD8+ gate)
% IL-2+ (in CD8+ gate)
Control
Anti-PD-1

Figure S6. Effects of PD-L1 overexpression in gastric epithelial cells on gastric tumorigenesis

(A) Experimental scheme depicting induction of gastric cancer in *R26*-PD-L1 control and Cre-expressing *R26*-PD-L1 mice with 5 cycles of MNU with or without *Helicobacter* infection.

(B) The percentage of $CD11b^{+}Gr\text{-}1^{-}F4/80^{+}$ macrophages in tumors from *R26*-PD-L1 (n = 5) and *Tff2*-Cre; *R26*-PD-L1 mice (n = 6) by flow cytometry.

(C-D) mRNA expression of chemokines (C) and growth factors/cytokines (D) in tumors from *R26*-PD-L1 and *Tff2*-Cre; *R26*-PD-L1 mice (n = 4/group).

(E) The percentage of $PD\text{-}L1^{+}$ cells in $EpCAM^{+}$ epithelial cells and $CD11b^{+}$ myeloid cells isolated from tumors in *R26*-PD-L1 (n = 5) and *Tff2*-Cre; *R26*-PD-L1 (n = 6) mice.

(F-G) Gross images (F) and tumor area measured (G) in *Tff2*-Cre; *R26*-PD-L1 mice treated with isotype control or anti-PD-1 at 24 weeks post-MNU for 6 weeks. Scale bars, 5 mm.

(H) The percentage of GzB^{+}, $LAMP\text{-}1^{+}$, Prf^{+}, $IFN\text{-}\gamma^{+}$, $TNF\text{-}\alpha^{+}$, and $IL\text{-}2^{+}$ cells in $CD8^{+}$ T cells isolated from *R26*-PD-L1 and *LysM*-Cre; *R26*-PD-L1 tumors (n = 3/group).

Data are represented as mean ± SEM. Student's t-test. $^{*}P < .05$; $^{**}P < .01$; $^{***}P < .001$; $^{****}P < 0.0001$.

A

		PD-L1			Total
		CPS < 1	1 ≤ CPS <10	CPS ≥ 10	
CD11b score	1	3 (10.7 %)	0 (0 %)	2 (7.1 %)	5 (17.9 %)
	2	4 (14.3 %)	9 (32.1 %)	6 (21.4 %)	19 (67.9 %)
	3	0 (0 %)	0 (0 %)	4 (14.3 %)	4 (14.3 %)
Total		7 (25 %)	9 (32.1 %)	12 (42.9 %)	28 (100%)

*P = .0219 by Fisher's exact test

B

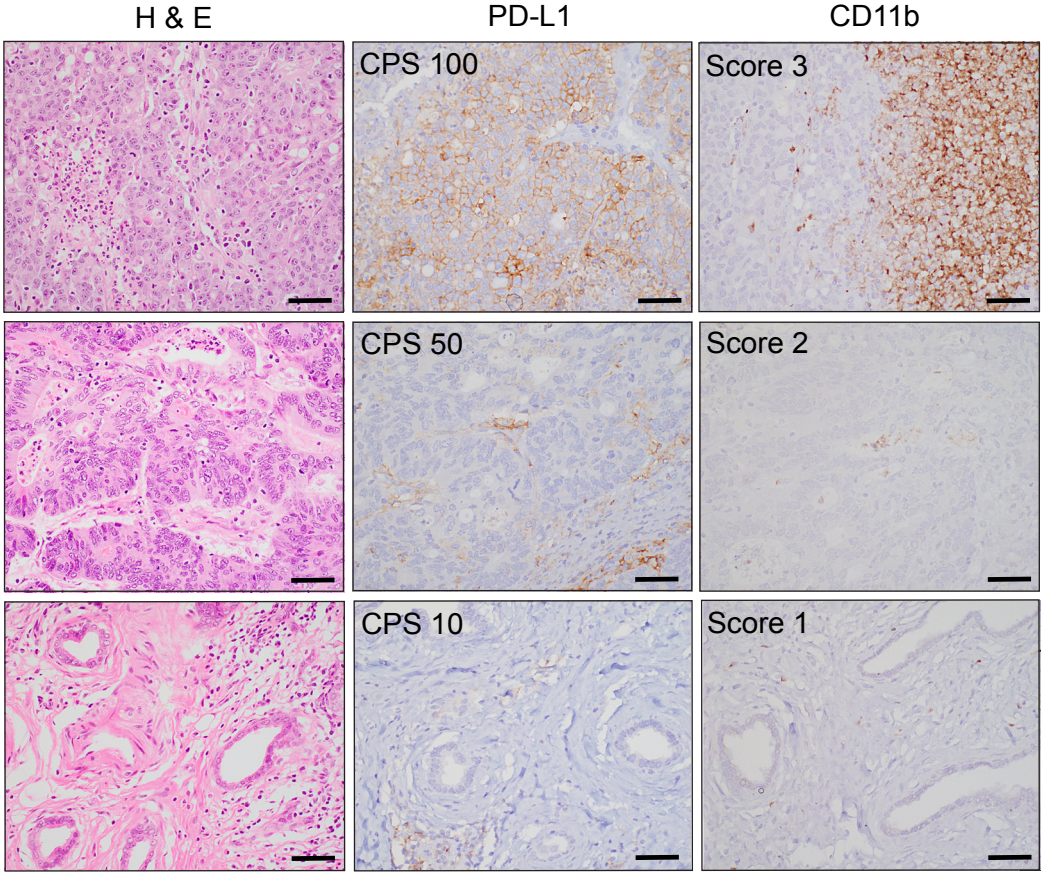

Figure S7. Expression of PD-L1 and CD11b in human gastric cancers
(A) Correlation between the expression levels of PD-L1 and CD11b in 28 human gastric cancer cases. Fisher's test. *P < .05.
(B) H&E, PD-L1, and CD11b staining in human gastric cancers. Scale bars, 50 μm.

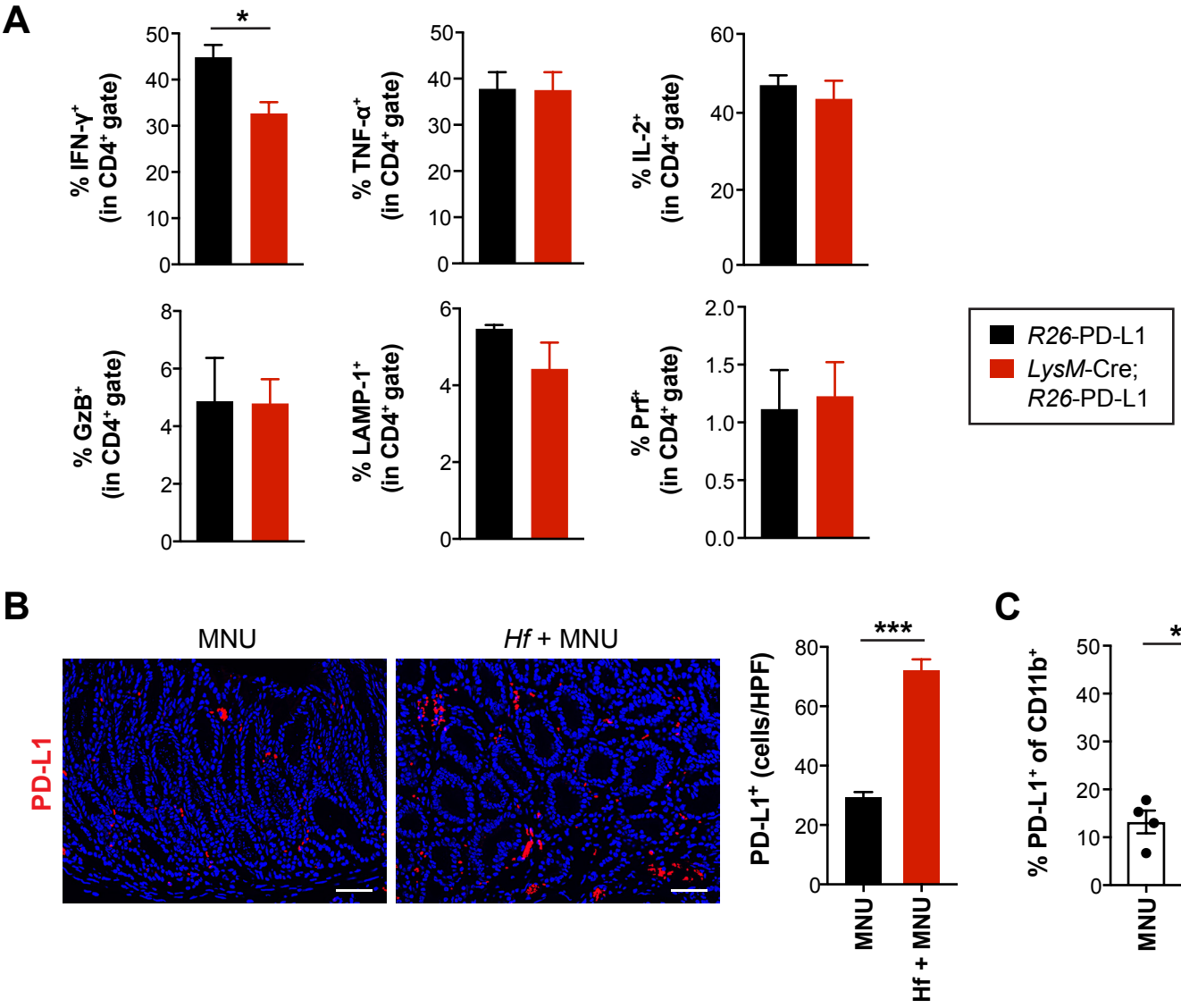

Figure S8. Effects of PD-L1 overexpression in myeloid cells on gastric tumorigenesis
(A) The percentage of IFN-γ$^+$, TNF-α$^+$, IL-2$^+$, GzB$^+$, LAMP-1$^+$, and Prf$^+$ cells in CD4$^+$ T cells isolated from tumors in MNU-induced *R26*-PD-L1 and *LysM*-Cre; *R26*-PD-L1 mice (n = 3/group).
(B) Immunofluorescence staining for PD-L1 on *R26*-PD-L1 tumors induced with MNU alone or in combination with *Helicobacter* and quantification of PD-L1$^+$ cells (n = 3/group).
(C) The percentage of PD-L1$^+$ cells in tumor CD11b$^+$ myeloid cells from MNU (n = 4) or *Hf*/MNU-induced (n = 6) *R26*-PD-L1 mice.
Data are represented as mean ± SEM. Student's t-test. *P < .05; ***P < .001.